Research Square

Preprints are preliminary reports that have not undergone peer review.
They should not be considered conclusive, used to inform clinical practice,
or referenced by the media as validated information.

PRMT2 Aggravates Pressure Overload–Induced Cardiac Remodeling by Promoting Endothelial-to-Mesenchymal Transition via methylation Snail1

Xianwei Fan
Department of Cardiology, Heart Center of Henan Provincial People's Hospital, Central China Fuwai Hospital, Central China Fuwai Hospital of Zhengzhou University

Xuejie Li
Department of Cardiology, Heart Center of Henan Provincial People's Hospital, Central China Fuwai Hospital, Central China Fuwai Hospital of Zhengzhou University

Juan Hu
Department of Cardiology, Heart Center of Henan Provincial People's Hospital, Central China Fuwai Hospital, Central China Fuwai Hospital of Zhengzhou University

Lijie Yan
Department of Cardiology, Heart Center of Henan Provincial People's Hospital, Central China Fuwai Hospital, Central China Fuwai Hospital of Zhengzhou University

Jintao Wu
Department of Cardiology, Heart Center of Henan Provincial People's Hospital, Central China Fuwai Hospital, Central China Fuwai Hospital of Zhengzhou University

Leiming Zhang
Department of Cardiology, Heart Center of Henan Provincial People's Hospital, Central China Fuwai Hospital, Central China Fuwai Hospital of Zhengzhou University

Jingjing Liu
Department of Cardiology, Heart Center of Henan Provincial People's Hospital, Central China Fuwai Hospital, Central China Fuwai Hospital of Zhengzhou University

Haitao Yang
haoyanghaitao123@163.com

Department of Cardiology, Heart Center of Henan Provincial People's Hospital, Central China Fuwai Hospital, Central China Fuwai Hospital of Zhengzhou University

---

Research Article

Keywords: Cardiac remodeling, Endothelial-to-mesenchymal transition, PRMT2, Snail1

Posted Date: April 17th, 2026

DOI: https://doi.org/10.21203/rs.3.rs-9213170/v1

License: This work is licensed under a Creative Commons Attribution 4.0 International License.
Read Full License

Additional Declarations: No competing interests reported.

Version of Record: A version of this preprint was published at Cardiovascular Drugs and Therapy on August 3rd, 2026. See the published version at https://doi.org/10.1007/s10557-026-07928-w.

Abstract

Purpose

Endothelial-to-mesenchymal transition (EndMT) plays a critical role in the development of cardiac remodeling under pathological stress. Emerging evidence suggests that protein methylation is an important post-translational modification involved in regulating EndMT. However, the role of protein arginine methyltransferase 2 (PRMT2), a key protein arginine methyltransferase, in modulating EndMT—particularly in the context of cardiac remodeling—remains poorly understood.

Methods

A transverse aortic constriction (TAC) mouse model was used to induce cardiac remodeling, and adeno-associated virus serotype 9 (AAV9) was administered to specifically silence PRMT2 in endothelial cells.

Results

We found that PRMT2 expression was significantly upregulated in cardiac endothelial cells following pressure overload. Endothelial-specific silencing of PRMT2 markedly attenuated cardiac hypertrophy, fibrosis, and EndMT in TAC mice. In vitro, PRMT2 knockdown in isolated murine cardiac microvascular endothelial cells alleviated TGF-β1–induced EndMT, while PRMT2 overexpression exacerbated it. Mechanistically, PRMT2 enhanced EndMT by promoting monomethylation of Snail1 and activation of the Snail signaling pathway. Importantly, endothelial-specific knockdown of Snail1 reversed the EndMT induced by PRMT2 overexpression.

Conclusion

These findings identify PRMT2 as a key epigenetic regulator of EndMT and cardiac remodeling, suggesting it may serve as a potential therapeutic target for heart failure.

1. Introduction

Cardiac remodeling is a pathological process characterized by cardiomyocyte hypertrophy, fibrosis, and vascular dysfunction, ultimately contributing to the development of heart failure[1]. Among the diverse cellular mechanisms involved, endothelial-to-mesenchymal transition (EndMT) has emerged as a critical contributor to cardiac fibrosis and structural remodeling[2]. During EndMT, endothelial cells lose their characteristic markers and acquire mesenchymal features, including increased motility and the expression of fibroblast-like proteins such as α-SMA and vimentin[3]. This phenotypic switch enables endothelial cells to participate in extracellular matrix deposition and fibrotic tissue formation[4]. Studies have demonstrated that EndMT is activated in response to various stressors, including pressure

overload, ischemia, and inflammation, and contributes significantly to myocardial stiffness and dysfunction[5]. Understanding the regulation of EndMT is therefore essential for developing targeted therapies to mitigate cardiac remodeling and progression to heart failure.

Protein arginine methylation is an essential post-translational modification that modulates a wide range of cellular processes, including transcriptional regulation, RNA processing, signal transduction, and epigenetic remodeling[6]. This modification is catalyzed by a family of enzymes known as protein arginine methyltransferases (PRMTs), which transfer methyl groups to the guanidino nitrogen atoms of arginine residues in target proteins[7]. In recent years, increasing evidence has highlighted the pivotal role of arginine methylation in cardiovascular biology and disease. Recently, Pyun JH et al found that cardiac specific PRMT1 ablation causes heart failure through Ca^{2+}/calmodulin-dependent protein kinase dysregulation[8]. Katanasaka Y reported that fibroblast-specific PRMT5 deficiency suppresses cardiac fibrosis and left ventricular dysfunction in male mice[9]. Among the protein arginine methyltransferase family, PRMT2 (Protein Arginine Methyltransferase 2) has gained increasing attention for its roles beyond traditional gene regulation. Unlike other PRMTs, PRMT2 possesses relatively weak enzymatic activity but exerts significant biological effects through both methylation-dependent and -independent mechanisms. Recent studies suggest that PRMT2 is involved in modulating inflammatory responses[10], lipid metabolism, and endothelial function[11]—all of which are key processes in the development of cardiovascular diseases. For instance, PRMT2 has been shown to inhibit NF-κB–mediated transcription, thereby suppressing vascular inflammation and atherosclerosis progression[12]. Despite these insights, the role of PRMT2 in myocardial remodeling and fibrosis remains poorly understood. In particular, its potential involvement in endothelial-to-mesenchymal transition (EndMT), a critical contributor to cardiac fibrosis, has yet to be fully elucidated.

In this study, we established a pressure overload–induced cardiac remodeling model using transverse aortic constriction (TAC) and silenced endothelial PRMT2 via AAV9. We found that PRMT2 expression was elevated in cardiac endothelial cells during remodeling. Endothelial-specific PRMT2 knockdown alleviated cardiac hypertrophy, fibrosis, and EndMT. Mechanistically, PRMT2 promoted EndMT by monomethylating Snail1 and activating the Snail pathway, while Snail1 silencing reversed the pro-EndMT effect of PRMT2. These findings reveal PRMT2 as a critical epigenetic regulator of EndMT and highlight its potential as a promising therapeutic target for preventing pathological cardiac remodeling and heart failure.

2. Methods

Animals

Experimental animals

Male C57BL/6J mice (8–10 weeks old, 22–25 g) were purchased from Beijing Huafukang Biotechnology Co., Ltd. (Beijing, China). All animals were housed under specific pathogen-free conditions with a 12-hour

light/dark cycle, controlled temperature (22 ± 2°C), and free access to standard chow and water. All experimental procedures were approved by the Institutional Animal Care and Use Committee of our university and conducted in accordance with the National Institutes of Health Guide for the Care and Use of Laboratory Animals.

AAV9 construction and delivery

To induce cardiac-specific PRMT2 knockdown, male C57BL/6J mice received a single tail vein injection of AAV9-TIE-shPRMT2 or control AAV9-ScRNA (Vigene Bioscience, Jinan, China; 60–80 μl, 5.0–6.5 × 10^{13} VG/ml) under 1.5–2% isoflurane anesthesia. Injections were performed two weeks before surgery[13]

Experimental Animals and Model

Pressure overload–induced cardiac remodeling was established by transverse aortic constriction (TAC) surgery as previously described[14]. Briefly, mice were anesthetized with isoflurane, and aortic constriction was performed using a 27-gauge needle to induce pressure overload. Sham-operated mice underwent the same procedure without ligation. Mice were randomly assigned to experimental groups and sham group.

Histological Analysis

Hearts were harvested, fixed in 4% paraformaldehyde overnight, and embedded in paraffin. Serial 5 μm-thick sections were prepared for staining. Sections were deparaffinized, rehydrated, and stained with hematoxylin for 5 minutes, followed by eosin for 2 minutes. After dehydration and mounting, sections were examined under a light microscope to evaluate myocardial morphology and cellular structure. For assessment of cardiac fibrosis, sections were stained with 0.1% picrosirius red solution for 1 hour. After washing, slides were dehydrated and mounted. Collagen deposition was visualized under polarized light microscopy and quantified using ImageJ software.

Immunofluorescence Staining

Paraffin sections were subjected to antigen retrieval by heating in citrate buffer (pH 6.0) for 15 minutes. After blocking with 5% bovine serum albumin (BSA) for 1 hour at room temperature, sections were incubated overnight at 4°C with primary antibodies against PRMT2 (Abcam, dilution 1:200), CD31 (Abcam, endothelial marker, 1:100), and α-SMA (Abcam, myofibroblast marker, 1:200). Following PBS washes, sections were incubated with appropriate fluorescently labeled secondary antibodies for 1 hour at room temperature in the dark. Nuclei were counterstained with DAPI. Images were captured using a fluorescence microscope and analyzed with ImageJ software.

Transcriptomic Profiling and Bioinformatics Analysis

Hieff NGS™ MaxUp Dual-mode Kit and DNA Selection Beads (YEASEN) were used to prepare mRNA libraries. Raw sequencing data were assessed for quality using FastQC and processed with Trimmoomatic. HISAT2 was employed to align clean reads to the reference genome followed by analysis with RSeQC and Qualimap for redundancy and uniformity checks. Expression levels were quantified as TPM (Transcripts Per Million) using StringTie, with differential expression analyzed via DESeq2, applying filters of qValue < 0.05. Differentially expressed genes were identified using a cutoff of |fold change| > 2. GO enrichment, KEGG pathway, and KOG classification analyses were performed using topGO and clusterProfiler.

Isolation and Culture of Cardiac Microvascular Endothelial Cells (CMECs)

CMECs were isolated from adult C57BL/6J mouse hearts as previously described[15]. Briefly, hearts were excised, rinsed in cold PBS to remove blood, and minced into small pieces (~ 1 mm^3). The tissue fragments were digested in a solution containing collagenase type II (1 mg/mL) and dispase (1 mg/mL) at 37°C for 45 minutes with gentle agitation. The resulting cell suspension was filtered through a 70 μm cell strainer and centrifuged at 300 × g for 5 minutes.

The cell pellet was resuspended and incubated with magnetic beads coated with anti-CD31 antibody (e.g., Miltenyi Biotec) for 30 minutes at 4°C. Endothelial cells were isolated using magnetic-activated cell sorting (MACS) according to the manufacturer's instructions. The purified CMECs were cultured on gelatin-coated dishes in endothelial growth medium (EGM-2, Lonza) supplemented with 10% fetal bovine serum (FBS) and endothelial growth supplements at 37°C in a humidified incubator with 5% CO_2.

The full-length mouse PRMT2 coding sequence was cloned into the adenoviral vector pAdTrack-CMV to generate Ad-PRMT2 (Vigene Bioscience, Jinan). Cardiac microvascular endothelial cells (CMECs) were infected with Ad-PRMT2 or Ad-GFP at a multiplicity of infection (MOI) of 50 for 48 hours before subsequent experiments. Small interfering RNAs (siRNAs) targeting mouse PRMT2 and Snail1, as well as scrambled negative control siRNA, were purchased from (Vigene Bioscience, Jinan). CMECs were transfected with siRNAs (final concentration 50 nM) using Lipofectamine RNAiMAX (Invitrogen) according to the manufacturer's instructions. Cells were then stimulated with recombinant human TGF-β1 (PeproTech) at a concentration of 10 ng/mL for 48 hours to induce EndMT.

Immunofluorescence Staining of CMECs

Cardiac microvascular endothelial cells (CMECs) grown on glass coverslips were fixed with 4% paraformaldehyde for 15 minutes at room temperature, followed by permeabilization with 0.3% Triton X-100 in PBS for 10 minutes. After washing with PBS, cells were blocked with 5% bovine serum albumin (BSA) for 1 hour at room temperature. Cells were then incubated overnight at 4°C with primary antibodies against E-Cadherin (Abcam, 1:200 dilution) and Vimentin (Abcam,1:200 dilution). Following three washes with PBS, cells were incubated with appropriate fluorescent secondary antibodies (e.g., Alexa Fluor 488 or 594 conjugated, 1:500 dilution) for 1 hour at room temperature in the dark. Nuclei

were counterstained with DAPI for 5 minutes. Coverslips were mounted onto slides with antifade mounting medium and imaged using a fluorescence microscope.

Western Blot Analysis

Cells or heart tissues were lysed in RIPA buffer supplemented with protease and phosphatase inhibitors (e.g., Roche). Protein concentrations were determined using the BCA protein assay kit (Pierce). Equal amounts of protein (20–40 μg) were separated by SDS-PAGE and transferred onto PVDF membranes (Millipore). Membranes were blocked with 5% non-fat milk in TBST for 1 hour at room temperature, then incubated overnight at 4°C with primary antibodies against PRMT2, Snail1, Twist1, E-Cadherin, Vimentin, GAPDH (Abam, 1:1000 dilution), MMA, ADMA, SDMA (Cell Signaling Technology, 1:1000 dilution). After washing, membranes were incubated with HRP-conjugated secondary antibodies for 1 hour at room temperature. Protein bands were detected using enhanced chemiluminescence (ECL) reagents (Thermo Fisher) and quantified by ImageJ software.

Quantitative Real-Time PCR (qPCR)

Total RNA was extracted from cells or tissue samples using TRIzol reagent (Invitrogen) according to the manufacturer's instructions. RNA purity and concentration were measured by a spectrophotometer (NanoDrop). Complementary DNA (cDNA) was synthesized using a reverse transcription kit (Takara PrimeScript RT reagent kit). qPCR was performed on a real-time PCR system (ABI 7500) using SYBR Green Master Mix (Applied Biosystems). Relative gene expression was calculated using the 2^−ΔΔCt method.

Co-immunoprecipitation (Co-IP) Assay

Cardiac microvascular endothelial cells (CMECs) were lysed in ice-cold IP lysis buffer (e.g., 50 mM Tris-HCl pH 7.4, 150 mM NaCl, 1% NP-40, 1 mM EDTA) supplemented with protease and phosphatase inhibitors. Lysates were cleared by centrifugation at 12,000 × g for 15 minutes at 4°C. Equal amounts of protein (500 μg–1 mg) were incubated overnight at 4°C with 2–5 μg of anti-PRMT2 antibody or anti-Snail1 antibody. Normal IgG was used as a negative control. Then, 30 μL of protein A/G agarose beads (Thermo Fisher) were added and incubated for 2–4 hours at 4°C with gentle rotation.

Wound healing assay

Cells were seeded at a density of 1 × 105 cells/well in 12-well plates. Upon reaching 90% confluence, cells were treated with TGF-β1 for 24 h and were serum-starved for 12h. After starvation, scratches were produced with 200μL pipette tips. Images were captured using a microscope.

Luciferase Reporter Assay

Cells were co-transfected with 500 ng of the firefly snail1 luciferase reporter plasmid containing the target promoter or 3'-UTR region, 50 ng of Renilla luciferase plasmid (pRL-TK) as an internal control, and

the indicated expression plasmids or siRNAs using Lipofectamine 3000 (Thermo Fisher Scientific) according to the manufacturer's instructions. After 24 to 48 hours of incubation, cells were lysed with Passive Lysis Buffer (Promega). Luciferase activities were measured using the Dual-Luciferase Reporter Assay System (Promega) on a luminometer (e.g., GloMax, Promega).

Statistical analysis

Data were confirmed to follow a normal distribution. Comparisons between two groups were performed using the unpaired Student's t-test. Differences between more than two groups were determined via a one-way ANOVA followed by the Student-Newman-Keuls (SNK) test. All data are expressed as the means ± SEMs. Statistical significance was set at $P < 0.05$.

3. Results

PRMT2 expression is upregulated in the heart and endothelial cells under pressure overload

To investigate the expression of PRMT2 under pressure overload, a mouse model of transverse aortic constriction (TAC) was established to induce cardiac pressure overload. Western blot analysis revealed that PRMT2 protein levels were significantly increased in heart tissue from mice subjected to TAC, compared to sham controls (Fig. 1A). However, when assessing isolated cell populations, PRMT2 expression remained unchanged in cardiomyocytes and fibroblasts (Fig. 1B-C), while it was markedly upregulated in cardiac endothelial cells following TAC (Fig. 1D).

To further investigate this finding, cultured cardiac microvascular endothelial cells (CMECs) were stimulated with TGF-β1 to mimic pathological stress conditions. Western blot analyses showed a significant increase in PRMT2 expression after TGF-β1 treatment (Fig. 1E). Consistently, immunofluorescence staining confirmed enhanced PRMT2 expression in TGF-β1-treated CMECs, further supporting its upregulation in endothelial cells under stress (Fig. 1F). These data suggest that pressure overload selectively induces PRMT2 expression in cardiac endothelial cells, but not in cardiomyocytes, and that pro-fibrotic stimulation with TGF-β1 is sufficient to increase PRMT2 expression in vitro.

Endothelial cell–targeted PRMT2 silencing attenuates pressure overload–induced cardiac hypertrophy and fibrosis

To determine the functional role of PRMT2 in cardiac remodeling, PRMT2 expression was silenced in vivo using an endothelial cell–targeted AAV9-shPRMT2 construct (Fig. 2A). Mice were subjected to TAC to induce pressure overload. Histological analysis revealed that PRMT2 silencing markedly attenuated cardiac hypertrophy, as shown by reduced heart weight/body weight (HW/BW), HW/tibia length (HW/TL), lung weight /BW (LW/BW), and LW/TL (Fig. 2B). In addition, HE and Picrosirius red staining demonstrated significantly decreased cardiomyocyte cross-sectional area and interstitial and perivascular fibrosis in PRMT2-silenced hearts following TAC (Fig. 2C-E). These findings indicate that

PRMT2 plays a key role in promoting pressure overload–induced cardiac hypertrophy and fibrosis, and that its silencing confers significant cardio-protection.

Endothelial-specific PRMT2 silencing preserves cardiac function and attenuates

EndMT in vivo

Echocardiographic analysis demonstrated that AAV9-shPRMT2 mice exhibited significantly improved cardiac function following TAC, with lower eft ventricular end-diastolic diameter (lvedd), left ventricular end-systolic diameter (LVESd), higher left ventricular ejection fraction (LVEF) and fractional shortening (FS) compared to control mice (Fig. 3A). qPCR analysis further confirmed reduced expression of hypertrophic (ANP, BNP, β-MHC) and fibrotic markers (collagen I, collagen III, α-SMA) in the PRMT2 knockdown group (Fig. 3B-C). Immunofluorescence staining of heart sections revealed a marked reduction in α-SMA (mesenchymal marker) and increased in co-expressing CD31 (endothelial marker) in PRMT2 knockdown mice compared with control mice 4 weeks after TAC (Fig. 3D). Additionally, Western blot analysis of heart tissue lysates demonstrated decreased expression of mesenchymal markers vimentin and increased expression of endothelial markers E-Cadherin in PRMT2 knockdown mice 4 weeks after TAC (Fig. 3E), further supporting the in vivo inhibition of EndMT following PRMT2 silencing.

PRMT2 promotes EndMT through interaction and monomethylation of Snail1

To elucidate the molecular mechanisms by which PRMT2 regulates EndMT, we first performed RNA sequencing on cardiac tissue from control and PRMT2-silenced mice following pressure overload. KEGG pathway enrichment analysis revealed that the most significantly altered pathways were related to fibrosis and EndMT (Fig. 4A-B), suggesting that EndMT maybe a key downstream process mediated by PRMT2. Western blot analysis showed that silencing PRMT2 led to a marked reduction in the expression of key EndMT-associated factors post TAC, including Snail1 and Twist1, (Fig. 4C). To explore the underlying mechanism, co-immunoprecipitation (Co-IP) assays demonstrated a direct interaction between PRMT2 and Snail1 in CMECs (Fig. 4D). To further investigate whether PRMT2 modulates Snail1 via methylation, we conducted lysine methylation assays. The results showed that PRMT2 specifically enhanced monomethylation of Snail1, while symmetric or asymmetric dimethylation was not significantly affected (Fig. 4E-G). Luciferase assay also found that PRMT2 increased the promoter activity of snail1, while PRMT2 siRNA down-regulated the transcriptional activity of snail1(Fig. 4H). These data suggest that PRMT2 regulates Snail1 function primarily through monomethylation. Together, these results demonstrate that PRMT2 promotes EndMT, at least in part, through interaction with and monomethylation of Snail1, thereby enhancing its activity and driving the EndMT program under stress conditions.

PRMT2 silencing attenuates TGF-β1–induced EndMT in cultured CMECs

To further validate the role of PRMT2 in EndMT, we performed in vitro experiments using primary cardiac microvascular endothelial cells (CMECs). Silencing PRMT2 with specific siRNA markedly reduced the

level of PRMT2 (Fig. 5A). CMECs were treated with TGF-β1 to induce EndMT in vitro. As expected, TGF-β1 stimulation significantly impaired cell viability, whereas PRMT2 silencing partially rescued cell viability (Fig. 5B), suggesting a protective effect of PRMT2 knockdown. Immunofluorescence staining and Western blot analysis revealed that TGF-β1 markedly increased the expression of the mesenchymal marker vimentin and decreased the expression of the endothelial marker E-cadherin. These changes were significantly attenuated upon PRMT2 silencing (Fig. 5C-D). Furthermore, qPCR analysis showed that TGF-β1 stimulation increased the transcription of key EndMT-related transcription factors, including Snail1, Snail2, Twist1, and Twist2. Notably, PRMT2 knockdown reduced the expression of all four genes (Fig. 5E). To assess the migratory behavior of CMECs, wound healing assays were performed. TGF-β1 significantly enhanced the migration of CMECs, consistent with a mesenchymal phenotype, while PRMT2 silencing reduced this migratory capacity (Fig. 5F).

PRMT2 overexpression exacerbates EndMT in vitro

To further confirm the role of PRMT2 in regulating EndMT, CMECswere transfected with Ad-PRMT2 to overexpress PRMT2 (Fig. 6A). TGF-β1 stimulation significantly impaired cell viability, whereas PRMT2 overexpression further reduced cell viability (Fig. 6B). Compared with control vector-transfected cells, PRMT2 overexpression significantly enhanced TGF-β1–induced EndMT, as demonstrated by a further decrease in the endothelial marker E-cadherin and an increase in mesenchymal markers vimentin (Fig. 6C). qPCR analysis showed that TGF-β1 stimulation increased the transcription of key EndMT-related transcription factors, including Snail1, Snail2, Twist1, and Twist2. Notably, PRMT2 overexpression increased the expression of all four genes (Fig. 6D). Together, these findings indicate that PRMT2 contributes to TGF-β1–induced EndMT and associated functional changes in endothelial cells, and its silencing effectively mitigates these effects.

Snail1 knockdown reverses PRMT2 overexpression–induced EndMT phenotype in vitro

To determine whether Snail1 mediates the pro-EndMT effects of PRMT2, CMECs were co-transfected with Ad-PRMT2 and Snail1-specific siRNA (Fig. 7A), followed by TGF-β1 stimulation. Cell viability was reduced in Ad-PRMT2 group but rescued in Ad-PRMT2 + Snial siRNA group (Fig. 7B). Immunofluorescence staining further confirmed that silencing Snail1 effectively prevented the phenotypic shift triggered by PRMT2 overexpression, with increased E-cadherin and decreased vimentin levels (Fig. 7C). qPCR analyses showed that Snail1 knockdown significantly abolished the PRMT2-induced upregulation of mesenchymal markers compared to PRMT2 overexpression alone (Fig. 7D). These results demonstrate that Snail1 is a critical downstream effector of PRMT2 in promoting EndMT, and that knockdown of Snail1 can effectively reverse PRMT2-driven EndMT phenotypes in endothelial cells.

4. Discussion

Endothelial-to-mesenchymal transition (EndMT) is increasingly recognized as a pivotal contributor to pathological cardiac remodeling under various stress conditions, including pressure overload[16]. During

EndMT, endothelial cells lose their specific markers and acquire mesenchymal and myofibroblast-like phenotypes, thereby contributing to myocardial fibrosis, impaired angiogenesis, and ventricular stiffening[16]. Recent studies have demonstrated that endothelial-derived fibroblast-like cells can account for a significant portion of activated fibroblasts in pressure overload–induced cardiac remodeling, highlighting the pathological relevance of EndMT in heart failure progression[3]. In our study, we identified protein arginine methyltransferase 2 (PRMT2) as a novel modulator of EndMT during pressure overload. PRMT2 expression was upregulated in cardiac endothelial cells under TAC, and its loss-of-function attenuated cardiac fibrosis and dysfunction. Mechanistically, PRMT2 promotes EndMT by facilitating the arginine methylation and stabilization of the key transcription factor Snail1, a master regulator of EndMT. This post-translational modification enhances Snail1's nuclear localization and transcriptional activity, thereby amplifying the expression of mesenchymal markers and repressing endothelial identity. Together, these findings suggest that PRMT2 accelerates cardiac remodeling by epigenetically sustaining EndMT through Snail1 methylation, providing a potential therapeutic target for preventing fibrotic progression in pressure overload–induced heart failure.

PRMTs are a family of enzymes that catalyze the methylation of arginine residues on histones and non-histone proteins, thereby regulating gene expression, signal transduction, and cellular differentiation[7]. In recent years, growing evidence has implicated several PRMT family members, particularly PRMT1, PRMT4, and PRMT5, in cardiovascular pathologies such as atherosclerosis, myocardial infarction, and cardiac hypertrophy[8, 17, 9, 18]. However, the role of PRMT2 in cardiovascular diseases remains relatively underexplored. Although PRMT2 has been reported to modulate inflammation and metabolism in other contexts[10], its involvement in cardiac remodeling and endothelial plasticity has not been clearly defined. Recent study found that PRMT2-mediated H3R8 asymmetric dimethylation (H3R8me2a) and promotes renal cell cancer tumorigenesis and metastasis[11]. PRMT2 was also reported to arginine methylation of BRD4 that regulates DNA damage and DNA repair[6]. Our study provides novel insights into the function of PRMT2 in methylation snail1. PRMT2 enhances the methylation and promoter activity of snail1, a critical transcriptional repressor of endothelial identity, leading to persistent activation of EndMT programs. These findings uncover a previously unrecognized role of PRMT2 in modulating endothelial cell phenotype and contribute to a deeper understanding of how epigenetic regulation of cell fate decisions influences cardiac remodeling.

The transcription factor Snail1 is a master regulator of EndMT[19]. It represses endothelial-specific genes such as CD31 and VE-cadherin while promoting the expression of mesenchymal markers including α-SMA, vimentin, and fibronectin, thereby driving the phenotypic conversion of endothelial cells[20]. In the cardiovascular system, Snail1 is activated in response to pro-fibrotic stimuli such as TGF-β, Notch, and Wnt signaling, and its persistent activation has been closely associated with pathological cardiac fibrosis and remodeling[21]. Importantly, the activity and stability of Snail1 are tightly regulated not only at the transcriptional level but also through various post-translational modifications including ubiquitination, phosphorylation, and methylation, that influence its nuclear localization and transcriptional potency[19]. In our study, we demonstrate that PRMT2 promotes EndMT by enhancing the methylation and stabilization of Snail1, leading to sustained activation of mesenchymal gene expression

and repression of endothelial identity. This finding underscores the central role of Snail1 in EndMT and reveals a novel epigenetic mechanism by which its activity is modulated in the context of cardiac stress. Targeting PRMT2-mediated regulation of Snail1 may thus represent a potential therapeutic avenue to limit EndMT-driven fibrosis and adverse cardiac remodeling.

In conclusion, our study identifies PRMT2 as a novel epigenetic regulator that aggravates pressure overload–induced cardiac remodeling by promoting endothelial-to-mesenchymal transition (EndMT). Mechanistically, PRMT2 enhances the arginine methylation of Snail1, a key transcription factor driving EndMT, thereby facilitating endothelial phenotypic transition and contributing to myocardial fibrosis. These findings not only expand our understanding of the molecular mechanisms underlying cardiac remodeling but also highlight the PRMT2–Snail1 axis as a potential therapeutic target for preventing or attenuating fibrosis-related heart failure.

Declarations

Acknowledgements

N/A.

Funding

The authors have no funding to declare.

5. Authors contribution

Haitao Yang conceptualized the study, designed experiments, and revised the manuscript. Xianwei Fan, Xuejie Li, Juan Hu, Lijie Yan, Jintao Wu completed the studies in vitro and in vivo. Xianwei Fan and Leiming Zhang contributed to data collection, analysis, interpretation. Xianwei Fan and Jingjing Liu wrote the original manuscript and designed the figures. All authors edited and collectively approved the final version of this manuscript.

6. Conflicts of interest

The authors declare that they have no known competing financial interests or personal relationships that could have appeared to influence the work reported in this paper.

7. Data availability

The data that support the findings of this study are available from the corresponding author upon reasonable request.

References

1. Nakamura M, Sadoshima J. Mechanisms of physiological and pathological cardiac hypertrophy. Nat Rev Cardiol. 2018;15(7):387–407. 10.1038/s41569-018-0007-y.
2. Singh A, Bhatt KS, Nguyen HC, Frisbee JC, Singh KK. Endothelial-to-Mesenchymal Transition in Cardiovascular Pathophysiology. Int J Mol Sci. 2024;25(11). 10.3390/ijms25116180.
3. Liu Y, Gao L, Zhao X, et al. Saikosaponin A Protects From Pressure Overload-Induced Cardiac Fibrosis via Inhibiting Fibroblast Activation or Endothelial Cell EndMT. Int J Biol Sci. 2018;14(13):1923–34. 10.7150/ijbs.27022.
4. Cheng W, Li X, Liu D, Cui C, Wang X. Endothelial-to-Mesenchymal Transition: Role in Cardiac Fibrosis. J Cardiovasc Pharmacol Ther. 2021;26(1):3–11. 10.1177/1074248420952233.
5. Zhang Z, Fang Z, Ge J, Li H. Endothelial-to-mesenchymal transition in cardiovascular diseases. Trends Mol Med. 2025. 10.1016/j.molmed.2025.05.002.
6. Liu L, Lin B, Yin S, et al. Arginine methylation of BRD4 by PRMT2/4 governs transcription and DNA repair. Sci Adv. 2022;8(49):eadd8928. 10.1126/sciadv.add8928.
7. Rakow S, Pullamsetti SS, Bauer UM, Bouchard C. Assaying epigenome functions of PRMTs and their substrates. Methods. 2020;175:53–65. 10.1016/j.ymeth.2019.09.014.
8. Pyun JH, Kim HJ, Jeong MH, et al. Cardiac specific PRMT1 ablation causes heart failure through CaMKII dysregulation. Nat Commun. 2018;9(1):5107. 10.1038/s41467-018-07606-y.
9. Katanasaka Y, Yabe H, Murata N, et al. Fibroblast-specific PRMT5 deficiency suppresses cardiac fibrosis and left ventricular dysfunction in male mice. Nat Commun. 2024;15(1):2472. 10.1038/s41467-024-46711-z.
10. Jin J, Bai H, Yan H, et al. PRMT2 promotes HIV-1 latency by preventing nucleolar exit and phase separation of Tat into the Super Elongation Complex. Nat Commun. 2023;14(1):7274. 10.1038/s41467-023-43060-1.
11. Li Z, Chen C, Yong H, et al. PRMT2 promotes RCC tumorigenesis and metastasis via enhancing WNT5A transcriptional expression. Cell Death Dis. 2023;14(5):322. 10.1038/s41419-023-05837-6.
12. Vurusaner B, Thevkar-Nages P, Kaur R, et al. Loss of PRMT2 in myeloid cells in normoglycemic mice phenocopies impaired regression of atherosclerosis in diabetic mice. Sci Rep. 2022;12(1):12031. 10.1038/s41598-022-15349-6.
13. Wu QQ, Liu C, Cai Z, et al. High-mobility group AT-hook 1 promotes cardiac dysfunction in diabetic cardiomyopathy via autophagy inhibition. Cell Death Dis. 2020;11(3):160. 10.1038/s41419-020-2316-4.
14. Wu Q, Yao Q, Hu T, et al. Dapagliflozin protects against chronic heart failure in mice by inhibiting macrophage-mediated inflammation, independent of SGLT2. Cell Rep Med. 2023;4(12):101334. 10.1016/j.xcrm.2023.101334.
15. Cai C, Guo Z, Chang X, et al. Empagliflozin attenuates cardiac microvascular ischemia/reperfusion through activating the AMPKalpha1/ULK1/FUNDC1/mitophagy pathway. Redox Biol. 2022;52:102288. 10.1016/j.redox.2022.102288.

16. Bischoff J. Endothelial-to-Mesenchymal Transition. Circ Res. 2019;124(8):1163–5. 10.1161/CIRCRESAHA.119.314813.
17. Zhang Z, Ding S, Wang Z, et al. Prmt1 upregulated by Hdc deficiency aggravates acute myocardial infarction via NETosis. Acta Pharm Sin B. 2022;12(4):1840–55. 10.1016/j.apsb.2021.10.016.
18. Wang Y, Yan S, Liu X, et al. PRMT4 promotes ferroptosis to aggravate doxorubicin-induced cardiomyopathy via inhibition of the Nrf2/GPX4 pathway. Cell Death Differ. 2022;29(10):1982–95. 10.1038/s41418-022-00990-5.
19. Fan M, Yang K, Wang X, et al. Lactate promotes endothelial-to-mesenchymal transition via Snail1 lactylation after myocardial infarction. Sci Adv. 2023;9(5):eadc9465. 10.1126/sciadv.adc9465.
20. Grande MT, Sanchez-Laorden B, Lopez-Blau C, et al. Snail1-induced partial epithelial-to-mesenchymal transition drives renal fibrosis in mice and can be targeted to reverse established disease. Nat Med. 2015;21(9):989–97. 10.1038/nm.3901.
21. Gomez Stallons MV, Wirrig-Schwendeman EE, Fang M et al. Molecular Mechanisms of Heart Valve Development and Disease. In: Nakanishi T, Markwald RR, Baldwin HS, Keller BB, Srivastava D, Yamagishi H, editors. Etiology and Morphogenesis of Congenital Heart Disease: From Gene Function and Cellular Interaction to Morphology. Tokyo2016. pp. 145 – 51.

Figures

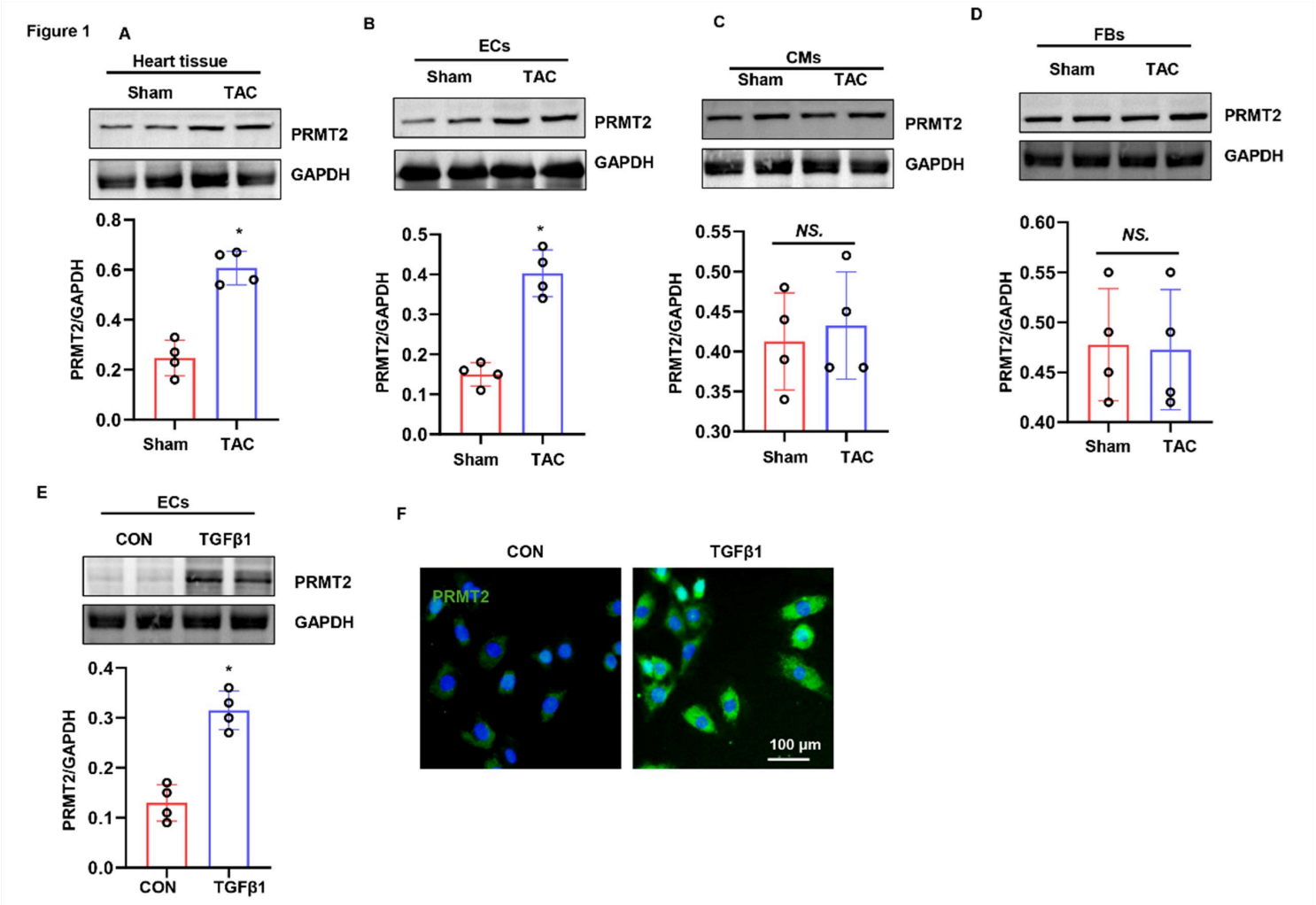


Figure 1

PRMT2 expression is upregulated in the heart and endothelial cells under pressure overload. A. Western blot analysis of PRMT2 protein levels in heart tissue from sham and TAC mice 4 weeks post surgery (n=4). B. Western blot analysis of PRMT2 protein levels in CMECs isolated from sham and TAC mice 4 weeks post surgery (n=4). C. Western blot analysis of PRMT2 protein levels in cardiomyocytes isolated from sham and TAC mice 4 weeks post surgery (n=4). D. Western blot analysis of PRMT2 protein levels in fibroblats isolated from sham and TAC mice 4 weeks post surgery (n=4). E. PRMT2 protein levels in CMECs treated with TGFβ1 (10 ng/mL, 48 h) (n=4). F. Immunofluorescence staining showing PRMT2 expression in primary cardiac microvascular endothelial cells (CMECs) stimulated with or without TGF-β1(10 ng/mL, 48 h) (n=5). ∗p < 0.05, and NS. indicates no significant difference.

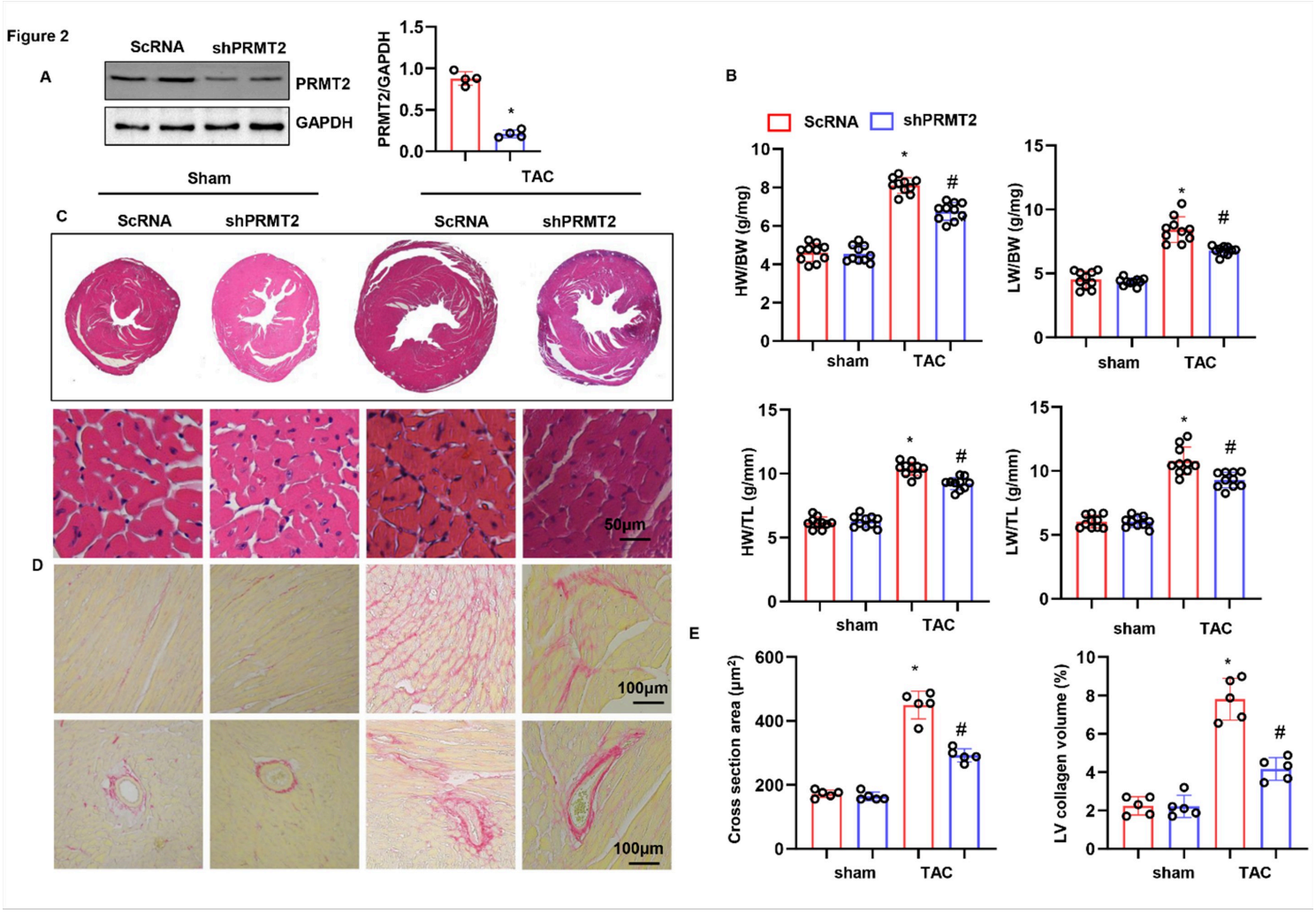


Figure 2

Endothelial cell–targeted PRMT2 silencing attenuates pressure overload–induced cardiac hypertrophy and fibrosis. A. PRMT2 protein levels in heart tissue from AAV9-shPRMT2 injection (n=4). B. Heart weight/body weight (HW/BW), heart weight /tibia length (HW/TL), lung weight /BW (LW/BW), and LW/TL ratios in each group 4 weeks post TAC (n=10). C. Representative hematoxylin and eosin (H&E) staining of heart sections(n=5). D. Representative picrosirius red (PSR) staining of cardiac fibrosis (n=5). E Quantification of cardiomyocyte cross-sectional area fibrotic area in PSR-stained sections. ∗p < 0.05: compared to the corresponding control group; #p < 0.05: compared to the ScRNA-TAC group.

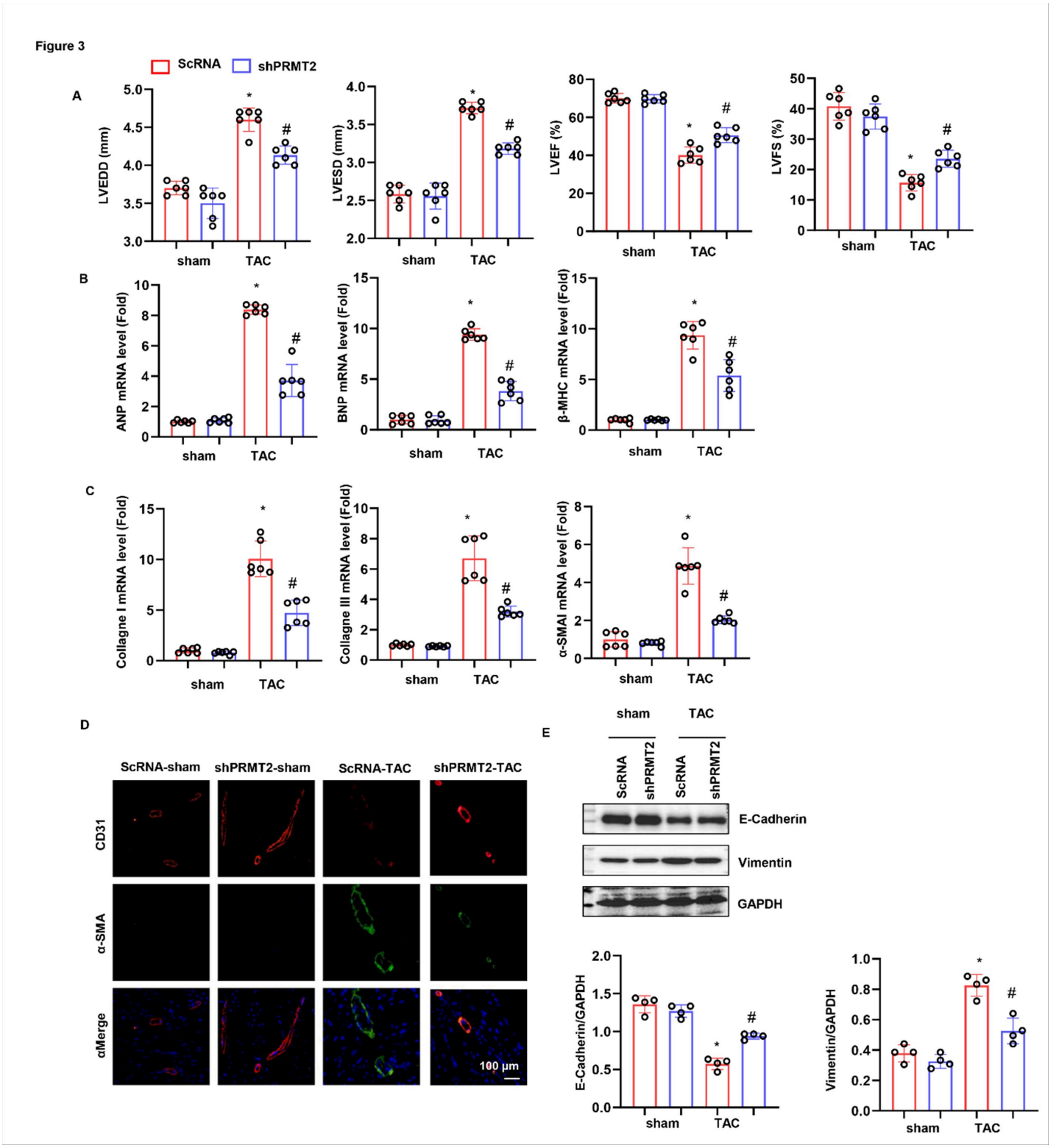


Figure 3

Endothelial-specific PRMT2 silencing preserves cardiac function and attenuates EndMT in vivo. A. Quantification of echocardiographic parameters: left ventricular ejection fraction (LVEF), left ventricular fractional shortening (LVFS), left ventricular end-diastolic diameter (LVEDD), and end-systolic diameter (LVESD) in each group 4 weeks post TAC (n=6). B-C. qPCR analysis of hypertrophic and fibrotic marker genes in heart tissue (n = 6). D. Representative images of immunofluorescence staining showing CD31

and α-SMA in heart tissue in each group 4 weeks post TAC (n=5). E. Protein level of E-Cadherin, and Vimentin in heart tissue in each group 4 weeks post TAC (n=4). ∗p < 0.05: compared to the ScRNA-sham group; #p < 0.05: compared to the ScRNA-TAC group.

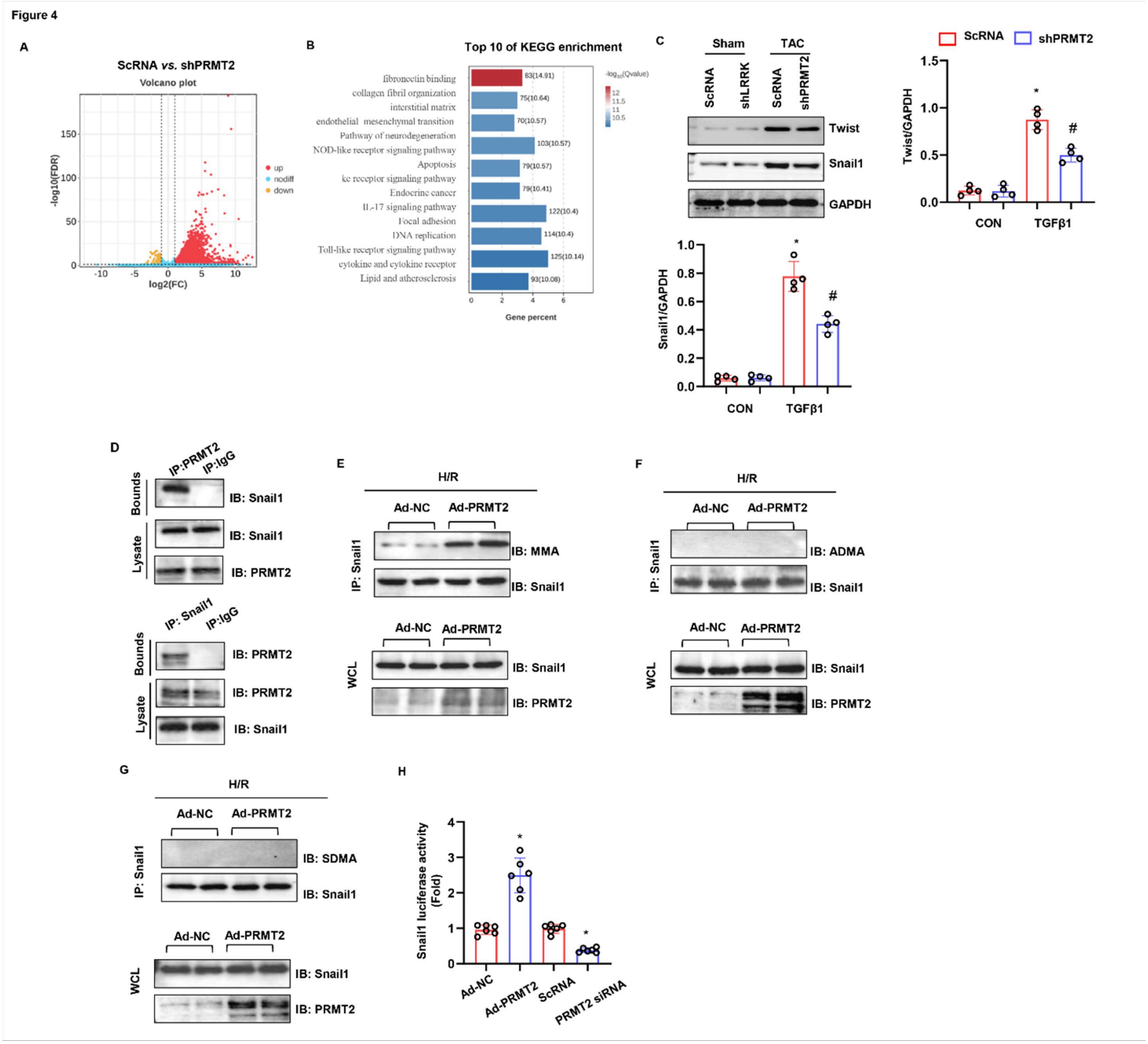


Figure 4

PRMT2 promotes EndMT through interaction and monomethylation of Snail1. A. Volcano plot of differentially expressed genes (DEGs) in cardiac tissue injected with AAV9-shPRMT2 (n=3). B. KEGG pathway enrichment analysis of DEGs (TOP10). C. Protein level of Twist, and Snail1 in heart tissue in each group 4 weeks post TAC (n=4). D. Co-IP of Snail1 and PRMT2 in CMECs. E. Co-IP of Snail1 and Monomethyl Arginine (MMA) in CMECs. F. Co-IP of Snail1 and Asymmetric Dimethyl Arginine (ADMA) in

CMECs. G. Co-IP of Snail1 and Symmetric Dimethyl Arginine (SDMA) in CMECs. H. Luciferase activity of snail1 in CMECs infected with Ad-PRMT2 or PRMT2 siRNA(n=6). ∗p < 0.05: compared to the corresponding control group; #p < 0.05: compared to the ScRNA-TAC group.

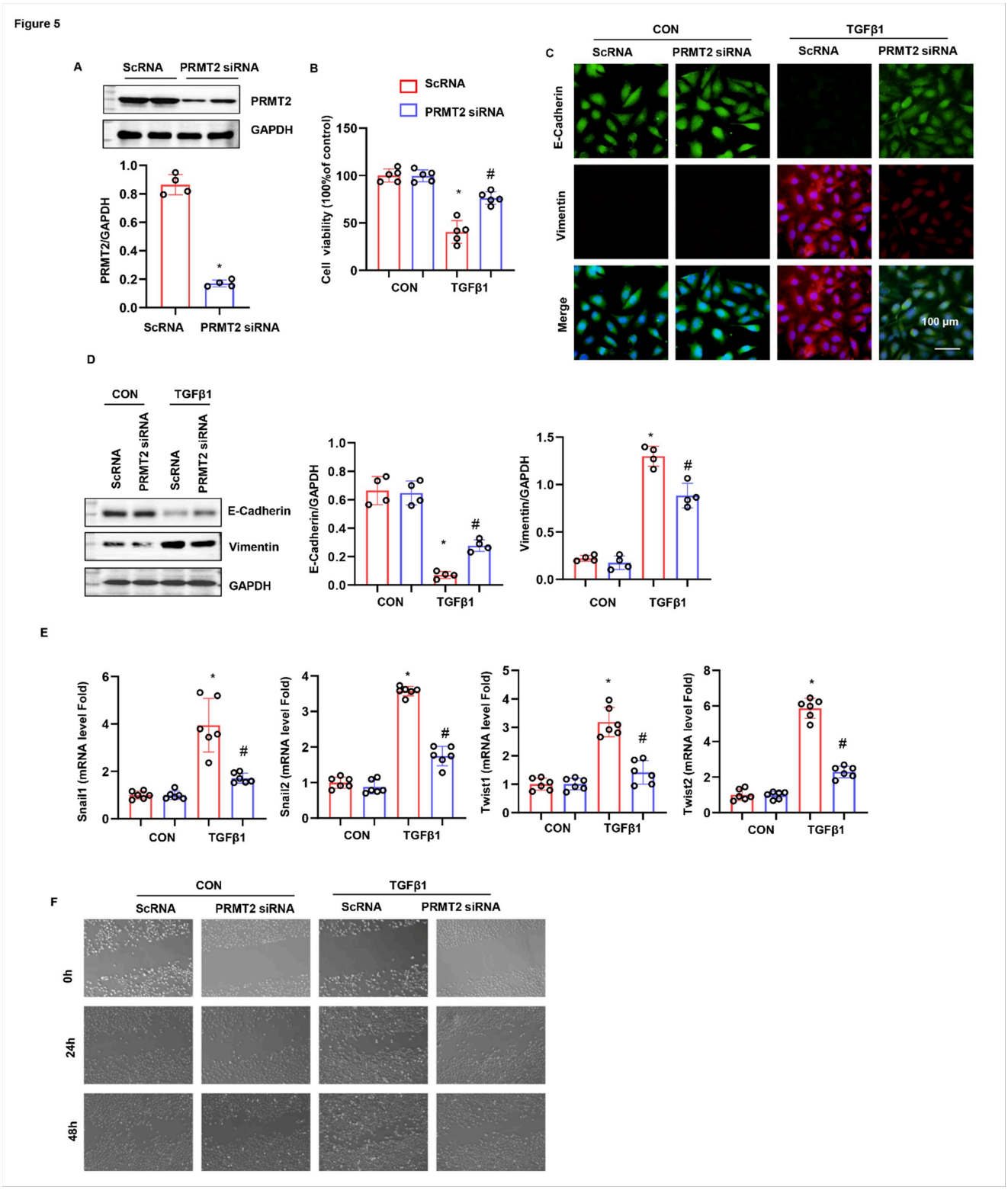


Figure 5

PRMT2 silencing attenuates TGF-β1–induced EndMT in cultured CMECs. A. Protein level of PRMT2 in CMECs infected with PRMT2 siRNA (n=4). B. Cell viability of CMECs treated with TGF-β1 (10 ng/mL, 48 h) (n=6). C. Immunofluorescence staining for E-cadherin (green) and Vimentin (red) in CMECs in each group (n=5). D. Western blot analysis and quantification of EndMT markers (E-cadherin, Vimentin) in CMECs in each group (n=4). E. qPCR analysis of EndMT-related gene expression following TGF-β1 stimulation (n = 6). F. Wound healing assay showing reduced cell migration upon PRMT2 silencing in TGF-β1–stimulated CMECs. ∗p < 0.05: compared to the corresponding control group; #p < 0.05: compared to the ScRNA-TGFβ1 group.

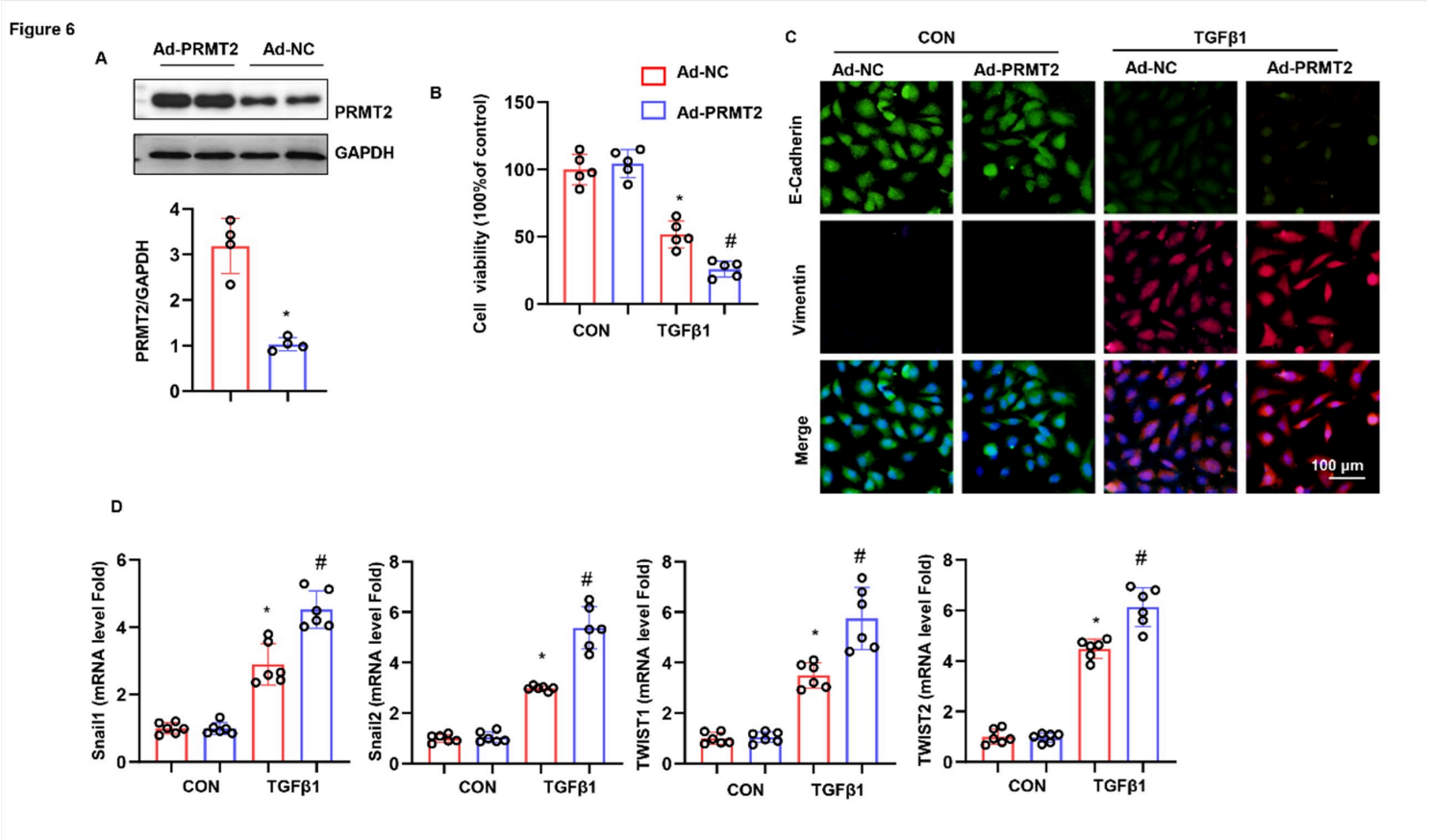


Figure 6

PRMT2 overexpression exacerbates EndMT in vitro.A. Protein level of PRMT2 in CMECs infected with Ad-PRMT2 (n=4). B. Cell viability of CMECs treated with TGF-β1 in each group (10 ng/mL, 48 h) (n=6). C. Immunofluorescence staining for E-cadherin (green) and Vimentin (red) in CMECs in each group (n=5). D. qPCR analysis of EndMT-related gene expression following TGF-β1 stimulation (n = 6). ∗p < 0.05: compared to the corresponding control group; #p < 0.05: compared to the Ad-NC-TGFβ1 group.

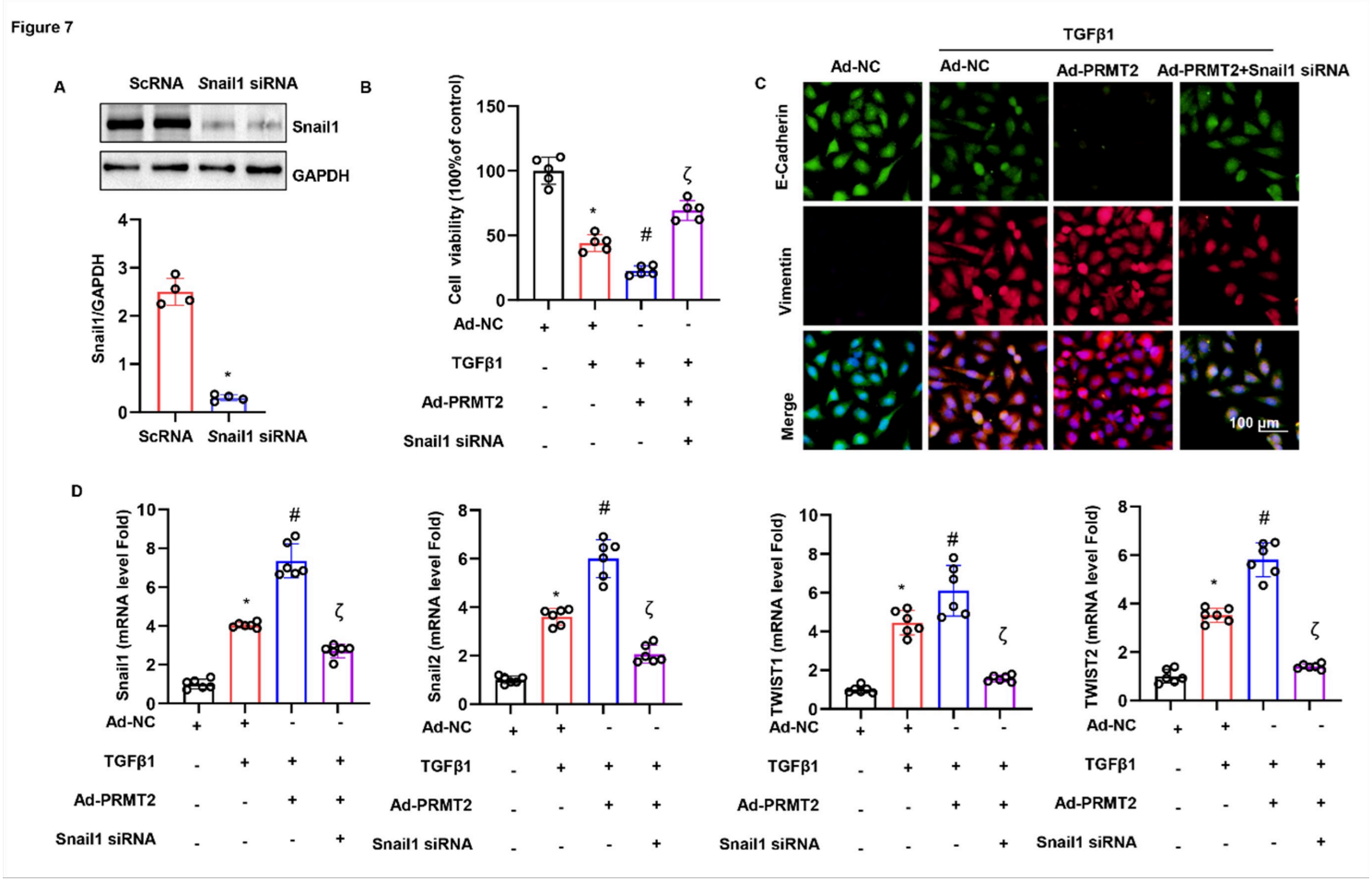


Figure 7

Snail1 knockdown reverses PRMT2 overexpression–induced EndMT phenotype in vitro. CMECs were infected with Ad-PRMT2 and snail1 siRNA then treated with TGF-β1(10 ng/mL, 48 h). A. Protein level of snail1 in CMECs infected with snail1 siRNA (n=4). B. Cell viability of CMECs treated with TGF-β1 in each group (10 ng/mL, 48 h) (n=6). C. Immunofluorescence staining for E-cadherin (green) and Vimentin (red) in CMECs in each group (n=5). D. qPCR analysis of EndMT-related gene expression following TGF-β1 stimulation (n = 6). ∗p < 0.05: compared to the corresponding control group; #p < 0.05: compared to the Ad-NC-TGFβ1 group; ζp < 0.05: compared to the Ad-PRMT2-TGFβ1 group.

Supplementary Files

This is a list of supplementary files associated with this preprint. Click to download.

- supplementaryfile.pdf